Biuletyn WAT
Vol. LXI, Nr 1, 2012

Evaluation of mechanical properties for pristine and defective carbon nanotubes and nanocomposites

ALEKSANDER MUC, MAŁGORZATA CHWAŁ,
ALEKSANDER BANAŚ

Cracow University of Technology, Institute of Machine Design,
24 Warszawska Str., 31-155 Cracow, Poland, olekmuc@mech.pk.edu.pl

Abstract. The existence of defects has a significant influence on mechanical properties of an analyzed structure. In the paper, a 3D nonlinear finite element model for single-walled carbon nanotubes with atom vacancy defects is proposed. The model is consistent with molecular mechanics' formulations. Assuming defects in CNTs, their influence on nanocomposites properties is discussed. The deformation process is described with the help of an iterative, non-linear procedure and the effective properties are evaluated with the use of the homogenization theory. The results are presented in the form of the strain-stress relations. The reduction by 19% for the failure stress and by 32% for the failure strain for defective CNT is predicted. It is observed that the failure strain for a pristine CNT is lower comparing with the case when a defective CNT reinforces nanocomposites.
Keywords: carbon nanotubes, nanocomposites, vacancy defects, numerical analysis

1. Introduction

Carbon nanotubes (CNTs) hold considerable promise as ultra-stiff high-strength fibers for the use in cabling and nanocomposites. The outstanding mechanical characteristics hold for nearly perfect CNTs. Several theoretical studies have reported CNT failure strains in the range of 20-30% and failure stresses usually in excess of 100 GPa. By contrast, the few direct mechanical measurements that have been reported indicate much lower values. Most attempts to resolve the theoretical-experimental discrepancies have concentrated on the possible role of defects in limiting peak strengths. If CNTs have defects in the crystal lattice, one can expect that due to their quasi-one-dimensional atomic structure even a small number

of defects will result in some degradation of their characteristics. The defects can appear at the stage of CNT growth and purification, or later on during device or composite production. Moreover, defects in CNTs can deliberately be created by chemical treatment or by irradiation to achieve the desired functionality. Therefore, possible defects in CNTs can be classified in the following manner:

— Point defects such as vacancies,
— Topological defects caused by forming pentagons and heptagons e.g. 5-7-7-5 defect — so-called Stone-Wales defects,
— Hybridization defects caused due to functionalisation.

Different approaches have been used to explore the role of vacancy defects in the fracture of CNTs under axial tension. In general, they can be divided into two groups: single- or two-atom vacancy defects Mielke et al. [1-5] or axisymmetric fracture patterns (defects) [6, 7]. However, the majority of existing works deals with the analysis of the Stone-Wales transformation that results in ductile fracture for nanotubes [8-11].

Significant challenges exist in both the micromechanical characterization of nanotubes and their composites and the modelling of the elastic and fracture behaviour at the nanoscale. In general, they include (a) complete lack of micromechanical characterization techniques for direct property measurement, (b) tremendous limitations on specimen size, (c) uncertainty in data obtained from indirect measurements, and (d) inadequacy in test specimen preparation techniques and lack of control in nanotube alignment and distribution. The above-mentioned problems and the description of nanocomposites fracture modelling are discussed in Refs [12-15].

In the present paper, the degradation in mechanical properties of defective CNTs and nanocomposites reinforced with imperfect CNTs is studied. The current work is the extension of the analysis conducted by Muc and Chwał [16-19].

It is worth to point out that the theoretical analysis of CNTs and nanocomposites fracture problems has adopted: the atomistic approaches (classical molecular dynamics (MD) and mechanics (MM)) and the continuum mechanics' approaches.

2. Interatomic potentials

To capture the essential feature of chemical bonding in graphite, Brenner [20] established an interatomic potential (called as the REBO potential) for carbon in the following form:

$$V^{TB}(r_{ij}) = V_R^{TB}(r_{ij}) - \overline{B}_{ij} V_A^{TB}(r_{ij}), \tag{1}$$

where V_R^{TB} and V_A^{TB} describe the repulsive and the attractive parts, respectively:

$$V_R^{TB}(r_{ij}) = f^{TB}(r_{ij})\frac{D_e^{TB}}{S^{TB}-1}e^{-\sqrt{2S^{TB}}\beta^{TB}\left(r_{ij}-R_{ij}\right)},$$
$$V_A^{TB}(r_{ij}) = f^{TB}(r_{ij})\frac{D_e^{TB}S^{TB}}{S^{TB}-1}e^{-\sqrt{\frac{2}{S^{TB}}}\beta^{TB}\left(r_{ij}-R_{ij}\right)}, \tag{2}$$

where r_{ij} is the distance between the atoms i and j, $f^{TB}(r_{ij})$ is the cut-off function, S^{TB} and β^{TB} are the constants. The parameter B_{ij} is given by:

$$B_{ij} = \left[1+\sum_{k(\neq i,j)} G\left(\theta_{ijk}\right)\right]^{-\delta}, \quad G(\theta) = a_0\left[1+\frac{c_0^2}{d_0^2}+\frac{c_0^2}{d_0^2+(1+\cos\theta)^2}\right],$$
$$\overline{B}_{ij} = \left(B_{ij}+B_{ji}\right)/2, \tag{3}$$

where θ_{ijk} is the angle between the bonds i-j and i-k. The material parameters adopted here as follows: D_e^{TB} = 0.9612 nN nm, S^{TB} = 1.22, β^{TB} = 21 nm^{-1}, R_{ij} = 0.139 nm, δ = 0.5, a_0 = 0.00020813, c_0 = 330, d_0 = 3.5.

For nanocomposites, the bonding between the nanotube and the matrix is in general modelled by van der Waals interactions. For simulations of van der Waals interactions, the Lennard-Jones "6-12" potential is adopted herein and it is written as:

$$V^{LJ}\left(r_{ij}\right) = 4\varepsilon\left[\left(\frac{\sigma}{r_{ij}}\right)^{12}-\left(\frac{\sigma}{r_{ij}}\right)^{6}\right], \tag{4}$$

For carbon atoms, the Lennard-Jones parameters are: ε = 0.0556 kcal/mole and σ = 3.4 Å [15].

3. Numerical model

3.1. Carbon nanotubes

In the present study, a numerical efficient formulation for modelling CNTs is presented based on the geometrically exact theory together with a finite element discretization incorporating atomistic potentials. This approach offers several advantages primarily related to the model's computational efficiency and to the possibility of a simple implementation into existing commercial FE codes.

Let us consider that the hexagon, which is the constitutional element of CNTs nano-structure, is simulated as structural element of a space-frame made of 3D beams. Of course, in the same way, the entire nanotube lattice may be modelled.

The simulation leads to the correspondence of the bond length C–C with the 3D beam element length L and with the element diameter d characterizing a circular cross-sectional area for the element. The linkage between molecular and continuum mechanics can be made by an appropriate definition of 3D beam mechanical properties.

Based on the energy equivalence between local potential energies in computational chemistry and elemental strain energies in structural mechanics, we can determine the tensile resistance, the flexural rigidity and the torsional stiffness for an equivalent beam. If the beam element is assumed to be of round section, then only three stiffness parameters, i.e., the tensile resistance EA, the flexural rigidity EI and the torsional stiffness GJ, need to be determined for deformation analysis. By considering the energy equivalence, a direct relationship between the structural mechanics parameters and the molecular mechanics force field constants can be established [15], i.e.:

$$\frac{E_i A_i}{r_i} = k_{ri}, \quad \frac{E_i I_i}{r_i} = k_{\theta i}, \quad \frac{G_i J_i}{r_i} = k_{ti}, \tag{5}$$

where k_{ri}, $k_{\theta i}$, and k_{ti} are the force field constants in molecular mechanics. They are indexed by the number of the beam occurring in the RVE for a given nanotube structure. For zigzag and armchair configurations, the RVE are plotted in Fig. 1.

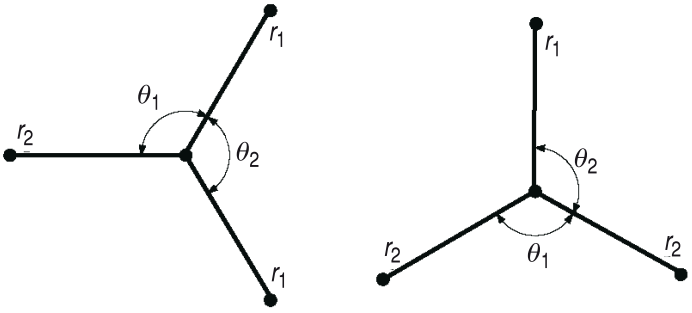

Fig. 1. Representative volume elements of a) armchair CNT and b) zigzag CNT [6]

Let us note that the present formulation is an extension of the models proposed in Refs [7, 15], and on the other hand, it incorporates special features of molecular mechanics models. In addition, it allows us to analyze large deformations of CNTs since the beam length L in Eq. (5) is replaced by an actual beam length r_i different for different beams in the RVE.

By comparing energies of the mechanical and molecular diatomic systems, the force constants k_{ri}, $k_{\theta i}$ can be derived. Using the interatomic potentials shown in Eqs (1) and (4), the stretching force that results from the bond elongation Δr_i

and the twisting moment that results from the bond angle variation $\Delta\theta_i$ can be calculated as follows:

$$F\left(\Delta r_i\right)=\frac{\partial V}{\partial r_i},\ M\left(\Delta\theta_i\right)=\frac{\partial V}{\partial\theta_i},\ \Delta r_i=r_i-r_{0i},\ \Delta\theta_i=\theta_i-\theta_{0i},\ i=1,2. \tag{6}$$

The derivatives in Eq. (6) are expanded in the Taylor series up to the first derivative (linear terms) only. However, the initial values r_{0i} and θ_{0i} are modified at each iteration step since, in fact, both the tensile forces and the twisting moments are nonlinear with respect to the bond length and to the bond angle, respectively. By assuming a circular beam cross-section with the diameter d_i, and setting $A_i=\pi d^2/4$, $I_i=\pi d^4/64$, Eqs. (5, 6) give:

$$d_i=4\sqrt{\frac{k_{\theta i}}{k_{ri}}},\ E_i=\frac{k_{ri}^2 r_i}{4\pi k_{\theta i}}. \tag{7}$$

Then, following the procedure of the finite element structural mechanics technique, the nanotube deformation under certain loading conditions can be readily solved. It is worth to note that the Young's moduli E_1 and E_2 are different even for the linear part of the stress-strain curve since the beam lengths r_i are different at each iteration step, and the force constants k_{ri} and $k_{\theta i}$ are nonlinear functions of r and θ, respectively, as the second derivatives of the interatomic potential.

3.2. Nanocomposites

The nanotube is modelled at the atomistic scale (see the previous section) whereas the polymeric matrix is much more convenient to treat as a continuum. For convenience, the CNTs are considered as straight fibers embedded in the composite. Therefore, for simulations of van der Waals interactions at the nanotube/polymer interface, a truss rod model is adopted — see Li, Chou [15].

It is assumed that the nanotube is embedded in the matrix (see Fig. 2a). Because the volume of the matrix is usually much greater than that of the reinforcement, the polymeric matrix is modelled as a continuum with the use of the classical 3D finite elements. At the nanotube/polymer interface, 3D finite elements are connected with the CNTs by a system of rods (see Fig. 2a). It is assumed that the rods at the nanotube/polymer interface have the length less than 0.4 nm. The Lennard-Jones potential describes the mechanical properties of the rods.

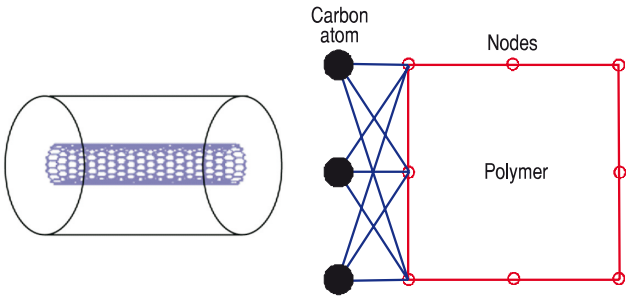

Fig. 2. Nanocomposite model: a) RVE and b) nanotube/polymer interface

3.3. Modelling of atom vacancies

Let us assume that a single atom is removed from the lattice being a pristine tube. Thus, 12-membered ring (two hexagons) can be reconstructed for instance to a five-membered ring and a nine-membered ring (see Fig. 3), and finally we obtain non-axisymmetric CNTs.

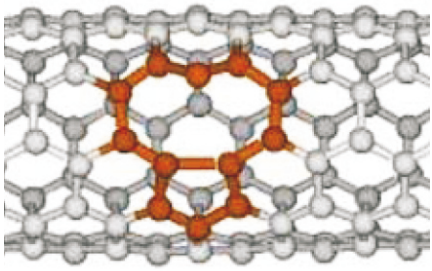

Fig. 3. The one-atom vacancy defect

Of course, using the similar approach, it is possible to model various types of defects.

4. Numerical results

In our approach, the Young's modulus of a material is defined as the ratio of longitudinal stress to longitudinal strain as obtained from a uniaxial tension test. Following this definition, the Young's modulus of CNTs has been calculated using the following equation:

$$E_{long} = \frac{\left\langle \sigma_{long} \right\rangle}{\left\langle \varepsilon_{long} \right\rangle}, \quad \left\langle \sigma_{long} \right\rangle = \sum_{k=1}^{N_{beams}} \sigma^{k}_{long}, \quad \left\langle \varepsilon_{long} \right\rangle = \sum_{k=1}^{N_{beams}} \varepsilon^{k}_{long}, \tag{8}$$

where $\langle \sigma_{long} \rangle / \langle \varepsilon_{long} \rangle$ is an average longitudinal stress/strain component computed as the sum of longitudinal components of each individual beams characterizing C–C bonds. Let us note that the above definition is more general than that described as the global in the first section and it is consistent with the homogenization theory. For nanocomposites, the average values are supplemented by the components obtained from the FE characterizing polymeric matrix and the nanotube/polymer interface (see Fig. 2). At each load step, corresponding to the increments of the axial displacements, the molecular mechanics' force field constants with the use of Eq. (6) as well as the beam geometrical and mechanical properties — Eq. (7) are evaluated in order to find the longitudinal stress components in individual beams. This iterative, non-linear procedure goes on to the prescribed end of the deformation process. The accuracy of modelling procedure depends on the number of load steps chosen. In order to maximize the accuracy of computational results, in each case, the displacement increment was chosen from convergence tests in which the convergence criterion was set equal to 2% of the maximal stress. Thereby, if between two sequential displacement increments a difference smaller than the 2% was achieved in the computed maximal stress, the larger displacement increment was finally adopted for the analysis.

Figure 4 shows the calculated stress-strain curves and Young's modulus of pristine and defective (with one-atom vacancy) carbon nanotubes from the present models. At the beginning, we have compared the Young's moduli of (5,5) armchair CNTs. The predicted initial Young's modulus of CNTs is 797 GPa and 708 GPa for the pristine and defective CNT, respectively, which agrees well with the experimental value and other theoretical values mentioned previously. Those values are strongly dependent on the form of the assumed interatomic potential and the form of defects.

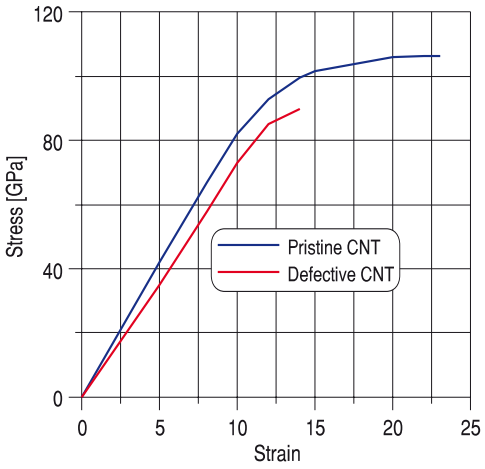

Fig. 4. Tensile stress-strain curves for pristine and defective (5,5) nanotube

The defects reduce the failure stresses by 19% and failure strains by 32%. It may reduce also buckling stresses for compressive loads since the defect considered may be treated as geometrical imperfection for cylindrical shells. It is also obvious that the reduction factor is significantly dependent on the form and magnitude of imperfections (the assumed type of defects).

For CNT with defect, considerable bond angle change is observed. Some of the initial bond angles deviate considerably from a perfect tube. Here, we calculate the critical strains of defect nucleation and fracture of CNTs embedded in a matrix by using our numerical/mechanics model. The interaction of CNTs in a composite may influence their deformation and fracture behaviours. The Young's modulus and Poisson's ratio of the matrix are taken as $E_m = 40$ GPa and $\nu_m = 0.2$, respectively. Figure 5 illustrates the stress-strain curves for nanocomposites reinforced by perfect and imperfect CNTs — the imperfection has the form presented in Fig. 3. It is found that when a CNT is placed in a composite, its critical strain of breaking will decrease (tab. 1).

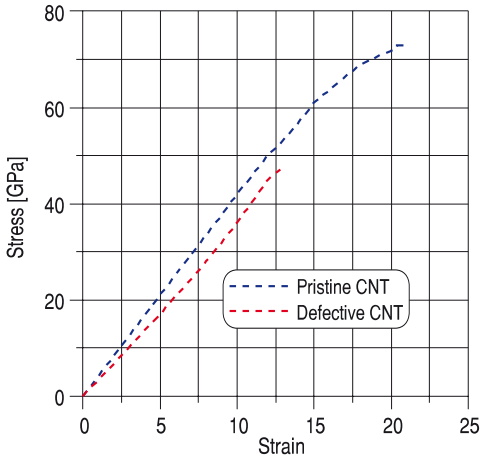

Fig. 5. Tensile stress-strain curves for pristine and defective nanocomposites reinforced by the armchair (5,5) nanotube (4% wt)

Table 1

Failure stresses and failure strains for pristine and defective structures

	CNT		Nanocomposites reinforced with	
	pristine	defective	pristine CNT	defective CNT
Failure stress [GPa]	108.1	90.1	73.5	47.6
Failure strain [%]	22.4	14.3	21.3	13.1

The critical strain of fracture of the (5,5) CNT is about 22.4 %, and it reduces to 21.3% after it is embedded in the composite. Similarly, the critical strain of

breaking of the defective (5,5) CNT decreases from 14.3% to 13.1% after it is put into the composite.

5. Conclusions

The reduction of the fracture stress and the fracture strain values might be attributed to the constraint effect of the matrix. A CNT embedded in a composite is less effective to release the energy, and becomes easier to fracture than that not embedded. In the present paper, we do not consider the fracture of the polymer matrix though in reality, most polymers cannot sustain such a high tensile strain. The above effects are also associated with the reduction of Young's modulus and the critical (failure) stresses. The values of critical strains and stresses are highly affected by the assumed values of the matrix Young's modulus. The critical strains decrease with the increase in the value E_m.

The paper was presented at the 2nd Polish Conference on Nano and Micromechanics (KKNM), Krasiczyn, 6-8 July, 2010.

Received November 19 2010, revised April 2011.

REFERENCES

[1] D. Troya et al., *Carbon nanotube fracture — differences between quantum mechanical mechanisms and those of empirical potentials*, Chem. Phys. Lett., 382, 2003, 133-141.

[2] S.L. Mielke et al., *The role of vacancy defects and holes in the fracture of carbon nanotubes*, Chem. Phys. Lett., 390, 2004, 413-420.

[3] K.M. Liew et al., *On the study of elastic and plastic properties of multi-walled carbon nanotubes under axial tension using molecular dynamics simulation*, Acta Mater., 52, 2004, 2521-2527.

[4] S.L. Mielke et al., *The effects of extensive pitting on the mechanical properties of carbon nanotubes*, Chem. Phys. Lett., 446, 2007, 128-132.

[5] S. Zhang et al., *Mechanics of defects in carbon nanotubes: Atomistic and multiscale simulations*, Phys. Rev. B, 71, 2005, 115403.

[6] W.H. Duan et al., *Molecular mechanics modelling of carbon nanotube fracture*, Carbon, 45, 2007, 1769-1776.

[7] K.I. Tserpes et al., *A progressive fracture model for carbon nanotubes*, Compos. Part B, 37, 2006, 662-669.

[8] M.B. Nardelli et al., *Brittle and ductile behaviour in carbon nanotubes*, Phys. Rev. Lett., 81, 1998, 4656-4659.

[9] J. Lu et al., *Analysis of localized failure of single-wall carbon nanotubes*, Comput. Mater. Sci., 35, 2006, 432-441.

[10] J. Song et al., *Stone-Wales transformation: Precursor of fracture in carbon nanotubes*, Int. J. Mech. Sci., 48, 2006, 1464-1470.

[11] P. Zhang et al., *An atomistic-based continuum theory for carbon nanotubes: analysis of fracture nucleation*, J. Mech. Phys. Sol., 52, 2004, 977-998.

[12] H.D. Wagner et al., *Stress-induced fragmentation of multiwall carbon nanotubes in a polymer matrix*, Appl. Phys. Lett., 72, 1998,188-190.

[13] O. Lourie et al., *Transmission electron microscopy observations of fracture of single-wall carbon nanotubes under axial tension*, Appl. Phys. Lett., 73, 1998, 3527-3529.

[14] D.-L. Shi et al., *Multiscale analysis of fracture of carbon nanotubes embedded in composites*, Int. J. Fract., 134, 2005, 369-386.

[15] C. Li et al., *Multiscale modelling of compressive behaviour of carbon nanotube/polymer composites*, Compos. Sci. and Technol., 66, 2006, 2409-2414.

[16] A. Muc, M. Chwał, *Mechanical models of composites based on carbon nanotubes* (in Polish), Kompozyty, 4, 2004, 432-438.

[17] A. Muc, M. Jamróz-Chwał, *Homogenization models for carbon nanotubes*, Mech. Comp. Mat., 40, 2004, 101-106.

[18] M. Chwał, *The homogenization of the mechanical properties of the composite materials reinforced with carbon nanotubes* (in Polish), PhD Thesis, Cracow University of Technology, 2007.

[19] A. Muc, *Design and identification methods of effective mechanical properties for carbon nanotubes*, Mat. Design, 31, 2010, 1671-1675.

[20] D.W. Brenner, *Empirical potential for hydrocarbons for use in simulating the chemical vapour deposition of diamond films*, Phys. Rev., B, 42, 1990, 9458-9471.

A. MUC, M. CHWAŁ, A. BANAŚ

Ocena własności mechanicznych nanorurek węglowych oraz nanokompozytów z defektami struktury i bez defektów

Streszczenie. Istnienie defektów znacząco wpływa na własności mechaniczne analizowanej struktury. W prezentowanej pracy przedstawiono numeryczne modele nanorurek węglowych z defektami struktury oraz ich wpływ na własności nanokompozytów. Rozpatrywane modele bazują na potencjałach oddziaływań międzyatomowych oraz metodzie elementów skończonych. Efektywne własności mechaniczne określono na podstawie teorii homogenizacji a proces deformacji opisano wykorzystując procedury nieliniowe. W wyniku przeprowadzonej analizy zaobserwowano 19% spadek naprężeń i 32% spadek odkształceń nanorurki węglowej w stosunku do struktury bez defektów. Efekt obniżenia własności sprężystych nastąpił także w analizowanych nanokompozytach wzmacnianych strukturami z defektami.

Słowa kluczowe: nanorurki węglowe, nanokompozyty, defekty, analiza numeryczna